Available online at www.sciencedirect.com
SCIENCE DIRECT
Developmental Biology 290 (2006) 265 – 276
DEVELOPMENTAL BIOLOGY
www.elsevier.com/locate/ydbio

# Solving an enigma: Arterial pole development in the zebrafish heart

Adrian C. Grimes [a,b,*], Harriett A. Stadt [b], Iain T. Shepherd [c], Margaret L. Kirby [a,b]

[a] *Medical University of South Carolina, Molecular and Cellular Biology and Pathobiology, 173 Ashley Avenue, Charleston, SC 29425, USA*
[b] *Duke University Medical Center, Department of Pediatrics (Neonatology), Bell Research Building, Trent Drive, Durham, NC 27710, USA*
[c] *Emory University, Department of Biology, 1510 Clifton Road, Atlanta, GA 30322, USA*

Received for publication 26 October 2005, accepted 3 November 2005
Available online 10 January 2006

**Abstract**

It is a widely held belief that the arterial pole of the zebrafish heart is unusual among models of comparative cardiogenesis. This is based, in part, on the report that the bulbus arteriosus undergoes a striated-to-smooth muscle phenotypic transition during development. An implication of this is that the zebrafish, a model almost ubiquitously accepted in other fields of comparative biology, may be poorly suited to the study of conotruncal abnormalities in human disease. However, while the use of atrioventricular-specific molecular markers has allowed extensive characterization of the development of the atrium and ventricle, the lack of any bulbus-specific markers has meant that this region of the zebrafish heart is poorly characterized and quite possibly misunderstood. We have discovered that the fluorescent nitric oxide indicator 4,5-diaminofluorescein diacetate (DAF-2DA) specifically labels the bulbus arteriosus throughout development from approximately 48 h post-fertilization. Therefore, using DAF-2DA and an immunohistochemical approach, we attempted to further characterize the development of the bulbus. We have concluded that no such phenotypic transition occurs, that contrary to current thinking, aspects of zebrafish arterial pole development are evolutionarily conserved, and that the bulbus should not be considered a chamber, being more akin to the arterial trunk(s) of higher vertebrates.


*Keywords:* Zebrafish; Cardiogenesis; Bulbus arteriosus; Arterial pole; Nitric oxide; Smooth muscle; DAF-2DA

## Introduction

Over two decades of extensive zebrafish research has validated its utility as a comparative biological model, and because of its rapid development and genetic tractability, *Danio rerio* has come to exemplify and legitimize the use of fish to model human disease (Epstein and Epstein, 2005). In particular, the species offers many advantages to the study of comparative cardiac morphogenesis and although there are fundamental differences between fully developed zebrafish and human hearts, at the heart-tube stage of development, they are morphologically almost indistinguishable (Fishman and Chien, 1997). It is widely reported that the teleost heart is comprised of four chambers, with blood flowing posterior to anterior through the sinus venosus, atrium, ventricle and bulbus arteriosus (Goodrich, 1930; Stainier et al., 1993; Bone et al., 1999; Hu et al., 2000, 2001; Simões et al., 2002). However, while there may be an implicit understanding that only the atrium and ventricle are 'true' cardiac chambers (e.g. Orr, 1982), confusion in the literature is such that the teleost heart has also been described variously as having two chambers (e.g. Schmidt-Nielsen, 1997) or three (Young, 1981), with the sinus venosus and bulbus arteriosus being occasionally described as 'subsidiary chambers' (e.g. Hickman et al., 1988) lacking in the mammalian heart (McCauley, 1971). It has therefore remained unclear how the bulbus should be designated, and this is by no means a trivial matter, as it is difficult to imagine how the four-chambered heart and parallel circulations of birds and mammals could have evolved from a three- or four-chambered, serial-circulation precursor. Although the adult bulbus lacks cardiac muscle and has characteristics that suggest it may originate from the ventral aorta (Lawson, 1979), an alternative theory is that it is of cardiac origin and may be an extension of the anterior portion of the heart, which subsequently loses its myocardial phenotype (Hu et al., 2000; Hu et

* Corresponding author. Duke University Medical Center, Department of Pediatrics (Neonatology), Bell Research Building, Trent Drive, Durham, NC 27710, USA. Fax: +1 919 668 1599.
*E-mail address:* grimes@duke.edu (A.C. Grimes).

0012-1606/$ - see front matter © 2005 Elsevier Inc. All rights reserved.
doi:10.1016/j.ydbio.2005.11.042

al., 2001; Guerrero et al., 2004). In either case, it is a fact that a disproportionate amount of zebrafish cardiac research has been concentrated on the atrium and ventricle at stages long before the bulbus is formed.

Fate-mapping experiments have facilitated the identification of atrioventricular progenitors in the lateral marginal zone of the early embryo prior to gastrulation (Keegan et al., 2004; Stainier et al., 1993). Furthermore, the use of atrial- and ventricular-specific molecular markers such as *ventricular myosin light chain* (*vmlc*) and *cardiac myosin light chain* (*cmlc*) has demonstrated that these two chambers are formed from distinct, but overlapping populations of cells (Keegan et al., 2004). These cardiac progenitors have been followed as they ingress through gastrulation and migrate with the lateral plate mesoderm towards the cranial midline, where they approach each other and fuse to form the primitive, beating heart tube by 24 h post-fertilization (hpf) (Stainier et al., 1993). The atrium and ventricle are both recognizable distinct structures within just 36 hpf.

In contrast, the bulbus arteriosus appears to be added to the heart after 48 hpf, at a stage when the atrium and ventricle are already formed and pumping blood through a rudimentary circulatory system. Because it forms so late, it is usually excluded from studies of the 'true' cardiac chambers, and a detailed analysis of its development has not been undertaken. Thus, as with other models used in the study of cardiogenesis (e.g. chick and mouse), confusion surrounds zebrafish arterial pole development.

One aspect that has seemed particularly enigmatic, and which both perpetuates the aforementioned confusion while also making the zebrafish unique among models of cardiogenesis, is the oft-cited report that the bulbus undergoes a transformation from a myocardial-covered heart chamber to a smooth muscle-covered arterial trunk during development (Hu et al., 2000). This observation has led to speculation about the processes involved (e.g. Rothenberg et al., 2003) and whether transdifferentiation, as proposed in other models such as chick and rat (Arguëllo et al., 1978; Ya et al., 1998), or remodeling through apoptosis, as shown in chick (Watanabe et al., 1998), is responsible for this change. However, the initial report was based on interpretation of histological data using a marker for striated muscle (myofilament-20, MF-20 Bader et al., 1982), but no marker for smooth muscle, and the timing of that transition was not documented sequentially.

We have discovered that the fluorescent nitric oxide (NO) indicator 4,5-diaminofluorescein diacetate (DAF-2DA) specifically labels the bulbus arteriosus from approximately 48 hpf and remains specific to the bulbus throughout development. Therefore, using DAF-2DA and multiple immunohistochemical markers for a basement membrane protein and both striated and smooth muscle, we attempted to better characterize the reported phenotypic change in both whole-mount and sectioned zebrafish embryos and discovered that the original report of a myocardial-to-smooth muscle transition was likely based on the misinterpretation of histological data. Here, we show that the bulbus arteriosus is never striated and that no phenotypic transition occurs. Furthermore, we demonstrate that aspects of zebrafish arterial pole development are evolutionarily conserved and that the bulbus should not be considered a chamber, being more akin to the arterial trunk(s) of higher vertebrates.

## Materials and methods

### *Zebrafish embryos*

Zebrafish were maintained following protocols described by Westerfield (1993) and Nusslein-Volhard and Dahm (2002). Eggs were generated from natural spawnings of AB or Tübingen wild-type (*wt*) fish, cleaned in fish water (300 μg/ml Instant Ocean Sea Salt in distilled water) and then maintained in blue water (fish water with 1 ng/ml methylene blue) at 28.5°C using standard protocols. In one experiment, embryos were generated by crossing *wt* fish with *cmlc*::DsRed2-nuc transgenics (Mably et al., 2003; a kind gift from Dr. Kenneth Poss [Duke University] with permission from Dr. Geoffrey Burns [Harvard Medical School]). Healthy embryos at various stages of development from 24 hpf to 30 days post-fertilization (dpf) (staged according to Kimmel et al., 1995) were selected for the experiments, transferred to a 35 mm petri dish and, when necessary, their chorions removed manually using watchmaker forceps. Thirteen adult fish (over 9 months old) were used for double-label immunohistochemistry experiments.

### *DAF-2DA labeling*

Live embryos were transferred from blue water directly into a 10 μM solution of DAF-2DA (Calbiochem, San Diego, CA) in fish water adjusted to pH 7.0 and incubated for 4 h in the dark at 28.5°C. Following incubation, embryos were either visualized in vivo or fixed in preparation for further immunohistochemical labeling as below. DAF-2DA is a membrane-permeable compound developed to detect the presence of NO in vivo (Kojima et al., 1998). After readily entering cells, DAF-2DA is hydrolyzed by endogenous esterases and converted to the membrane-impermeable 4,5-diaminofluorescein (DAF-2). This in turn reacts with NO in the presence of oxygen to yield the highly fluorescent adduct triazolofluorescein (DAF-2T), with fluorescence being linearly correlated (up to saturation levels) with the concentration of the compound.

### *Immunohistochemistry*

Initial double-labeling experiments were performed without the use of DAF-2DA. Embryos were anaesthetized in 0.016% tricaine and fixed for 50 min using 2% paraformaldehyde in PBS (pH 7.4). Following fixation, embryos were rinsed in PBS, placed in blocking solution (PBS with 10% [v/v] sheep serum; 2 mg/ml BSA; 0.2% [w/v] saponin) for 50 min and then incubated in 1:20 monoclonal antibody MF-20 supernatant (Developmental Studies Hybridoma Bank, University of Iowa, IA) in antibody buffer (PBS with 0.2% saponin; 2% milk) for 2 h at room temperature. After rinsing in PBS, embryos were incubated for 2 h at room temperature in the dark with 1:500 AlexaFluor 568 goat anti-mouse $IgG_{2b}$ secondary antibody (Molecular Probes, Eugene, OR) in antibody buffer as before. After a further rinse in PBS, embryos were incubated overnight at 4°C in the dark with 1:1000 anti-smooth muscle α-actin monoclonal antibody conjugated to FITC (Sigma) in antibody buffer. This protocol allowed visualization of striated muscle in red and smooth muscle in green. Prior to whole-mount visualization, embryos were dehydrated in methanol series and cleared in 2:1 benzyl benzoate:benzyl alcohol.

Four adult fish were fixed overnight at 4°C in 4% paraformaldehyde, their hearts exposed by opening the pericardial cavity and double-labeled as above. Following labeling, the hearts were excised from the fish and imaged.

For DAF-2DA experiments, after incubation in a solution of the reagent as above, embryos were rinsed in fish water, anesthetized in 0.016% tricaine and fixed for 30 min using 2% paraformaldehyde in PBS (pH 7.4). Following fixation, embryos were rinsed in PBS, placed in blocking solution as above for 50 min and then incubated in antibody buffer for 2 h at room temperature with primary antibodies as follows. Either 1:20 monoclonal antibody MF-20

supernatant; or 1:20 anti-tropomyosin monoclonal antibody CH-1 supernatant (Developmental Studies Hybridoma Bank, University of Iowa, IA); or 1:1 anti-sarcomeric myosin monoclonal antibody NA-4 supernatant (Developmental Studies Hybridoma Bank, University of Iowa, IA); or 1:1000 anti-smooth muscle MLCK monoclonal antibody, clone K36 (Sigma); or 1:100 anti-smooth muscle MHC IgG (Biomedical Technologies, Stoughton, MA); or 1:1000 anti-smooth muscle α-actin, clone 1A4 (Sigma). After rinsing again in PBS, embryos were incubated for 2 h at room temperature in the dark with either 1:500 AlexaFluor 568 goat anti-mouse IgG (H + L) or 1:500 AlexaFluor 568 goat anti-rabbit IgG (H + L) secondary antibodies (Molecular Probes, Eugene, OR) in antibody buffer as before. Prior to visualization, embryos were dehydrated in methanol series and cleared in 2:1 benzyl benzoate:benzyl alcohol. This protocol allowed for visualization of either striated or smooth muscle structures in red and DAF-2DA reactivity in green.

### *Frozen sections*

After labeling with anti-striated muscle/anti-smooth muscle antibodies, embryos at various developmental stages were rinsed in PBS, transferred to 5% (w/v) sucrose/PBS at 4°C for 4 h and then left at 4°C overnight in 20% (w/v) sucrose/PBS. Embryos were infiltrated with 7.5% (w/v) gelatin (Sigma G2500)/15% (w/v) sucrose/PBS at 38°C for 4 h and then embedded in disposable moulds by cooling the same mixture to room temperature. Moulds were discarded, and the congealed gelatin/sucrose was trimmed and mounted on a cryostat chuck with OCT compound and frozen for 1 min in dry-ice-chilled isobutane. Embryos were sectioned at 12 μm on a Leica CM3050S cryostat, mounted on glass slides and allowed to dry at room temperature. Slides were soaked in PBS for 30 min at 38°C to clear the gelatin and then coverslipped using warmed ProLong Gold Antifade Reagent with DAPI (Molecular Probes, Eugene, OR) to allow visualization of cell nuclei.

### *Paraffin embedding and sectioning*

Following whole-mount visualization of DAF-2DA and anti-striated muscle/anti-smooth muscle reactivity, selected embryos were transferred directly from 2:1 benzyl benzoate:benzyl alcohol to xylenes and allowed to equilibrate for 5 min prior to being placed in paraffin at 60°C. Embryos were embedded in disposable plastic moulds and allowed to cool before being sectioned at 8 μm on a Leica RM2155 microtome, mounted on glass sides and allowed to dry overnight in the dark. The following day, slides were heated to 60°C in an oven, placed in xylenes for 5 min, rehydrated through ethanol series to water and coverslipped using warmed ProLong Gold Antifade Reagent with DAPI.

### *Additional histology and immunohistochemistry*

Nine adult fish, three of which had been incubated overnight in a solution of DAF-2DA, were fixed overnight at 4°C in 4% paraformaldehyde, their hearts excised and prepared for paraffin embedding and sectioning as above. One subset of sections was stained with hematoxylin, eosin and Mallory's trichrome stain using standard histochemistry protocols, and coverslipped using Cytoseal-60 (Richard Allan Scientific, Kalamazoo, MI). A second subset was double-labeled with MF-20 and polyclonal anti-laminin antibody (L9393, Sigma) after being predigested with 0.5% papain (Sigma) in 0.02 M phosphate buffer (pH 4.7) for 10 min at 37°C, rinsed in Tris/Tween (0.1 M Tris [pH 7.6]/0.1% Tween 20) and pre-blocked using Tris/Tween/2% FBS. Sections were serially incubated for 1 h each with 1:20 MF-20, 1:200 AlexaFluor 568 goat anti-mouse IgG (H + L) secondary antibody, 1:1000 L9393 anti-laminin and 1:200 AlexaFluor 488 goat anti-rabbit IgG (H + L) secondary antibody. Between each incubation, slides were rinsed in Tris/Tween and blocked in Tris/Tween/FBS. The remainder of the sections (those showing DAF-2DA reactivity) was labeled with 1:20 MF-20 using similar protocols as above. Following staining, sections were rinsed in water and coverslipped using warmed ProLong Gold Antifade Reagent with DAPI.

### *DAF-2DA reactivity in chick*

Fertilized chicken eggs, obtained from the Gold Kist Hatchery, Siler City, NC, were incubated at 37°C and 70% humidity in a forced-draft incubator. Embryos were revealed by cutting a small (1″ × 1/2″) opening in the egg. Approximately, 2 μl of a 5 mM DAF-2DA solution was injected into a vitelline vein of embryos at HH stages 24–34 (Hamburger and Hamilton, 1951) using back-filled pulled glass capillaries. The eggs were sealed using Scotch-tape and then incubated for an additional 24 h before the hearts were dissected, fixed overnight in 4% paraformaldehyde, labeled with MF-20 using similar protocols as above and then placed in PBS for visualization.

### *Imaging*

Whole-mount embryos were visualized using a Leica MZ FLIII microscope equipped with a Q-Imaging Retiga 1300i camera and EXFO X-cite 120 Fluorescence Imaging System. Paraffin and frozen sectioned embryos were visualized using a Leica DM RAZ microscope equipped similarly with camera and fluorescence imaging system. Overlay images were generated using Improvision Openlab software or Adobe Photoshop.

## Results

### *The zebrafish bulbus arteriosus is never striated*

Histological analysis has revealed that the adult zebrafish bulbus contains a considerable volume of smooth muscle (Hu et al., 2001), and we confirmed this by anti-smooth muscle actin labeling of several adult hearts (Fig. 1). However, although in early-stage embryos we found that both skeletal muscle and myocardium were clearly marked by MF-20 from 24 hpf, none of the smooth muscle markers labeled any cardiac region during stages of development when the bulbus was

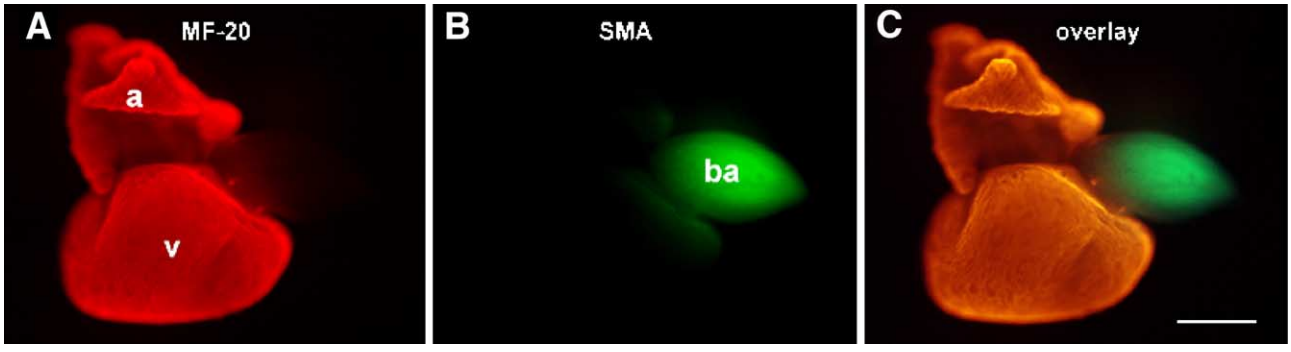


Fig. 1. Confirmation of smooth muscle phenotype in the adult zebrafish bulbus arteriosus. Whole-mount immunolabeling using anti-myosin MF-20 (red) and anti-smooth muscle alpha-actin (green); lateral view, dorsal to the top, cranial to the right. a—atrium. ba—bulbus arteriosus. v—ventricle. Scale bar—500 μm.

being added to the heart (Fig. 2). Smooth muscle marker reactivity was seen in the bulbus at various late stages, but only after it was already formed, and the timing of that reactivity depended on the marker being used. In our experiments, anti-smooth muscle myosin light chain kinase (sMLCK) was the earliest marker to label smooth muscle in the bulbus and was identifiable after approximately 20 dpf (data not shown). However, although we were unable to show the presence of smooth muscle in the early developing bulbus using immuno-histochemistry, we also discovered in all embryos examined (from 24 hpf through to over 30 dpf) that neither was there any evidence of striated muscle in this structure at any stage of development, as MF-20 labeling did not extend beyond the lip of the ventricle. Fig. 2A shows that, at 36 hpf, striated muscle is limited to the atrium and ventricle, and frozen sagittal sections of immunolabeled embryos at various developmental stages also illustrate that the bulbus is never striated (Figs. 2B–D). This lack of myocardium in the bulbus arteriosus was confirmed by the use of two additional striated muscle markers, CH-1 against tropomyosin (Figs. 2E, F) and NA-4 against sarcomeric myosin (data not shown). However, because a phenotypic transition had been previously reported (Hu et al., 2000) and the bulbus described as a ring of MF-20-positive cardiomyocytes distal to the ventricle in transverse-sectioned early embryos, we attempted to duplicate that data and discovered that this ring was in fact a narrow band of striated myocardium at the lip of the ventricle in a region of the heart surrounding and supporting the bulboventricular valve. For example, in a 5 dpf embryo, MF-20 reactivity did not extend further than approximately 16 μm (2 × 8 μm sections) distal to the valve (Fig. 3), and this region does not correspond to the wall of the bulbus.

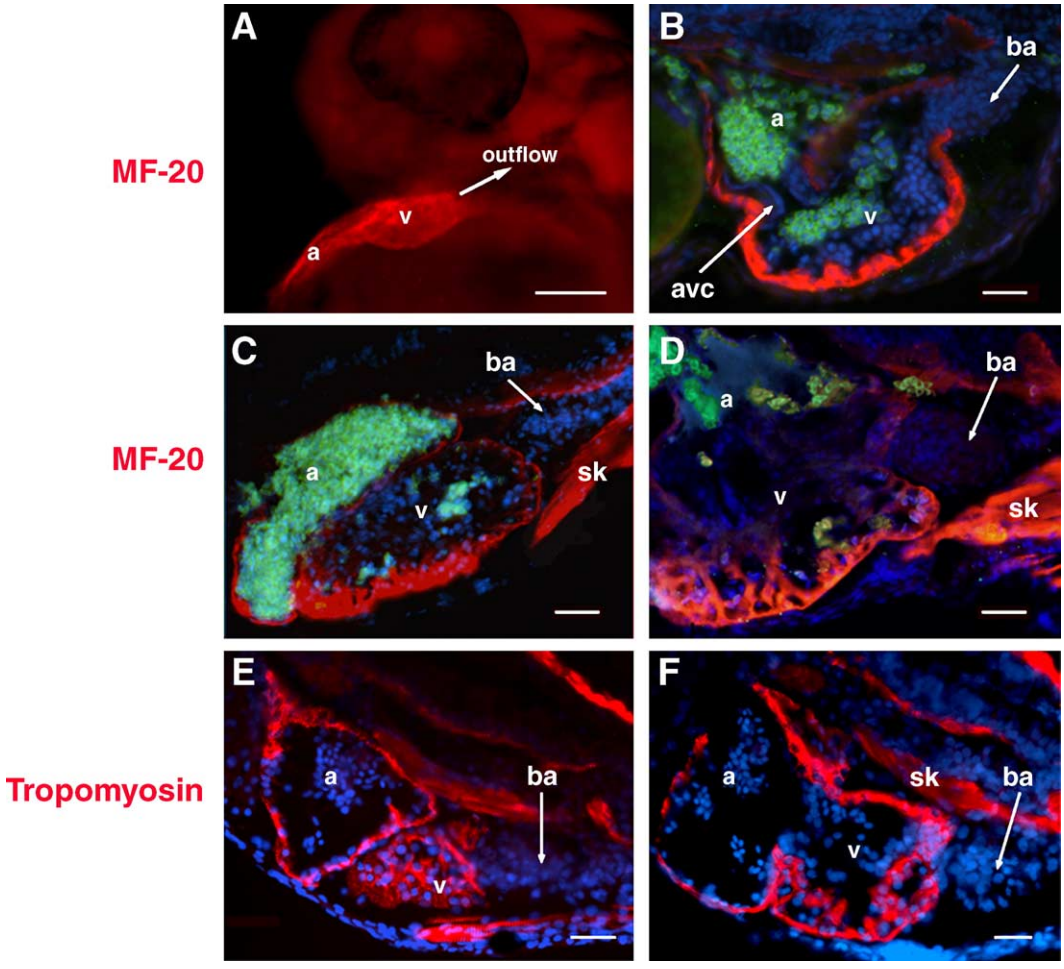


Fig. 2. The zebrafish bulbus arteriosus is non-striated throughout development. Immunolabeled whole-mount (A) and sagittal sections (B–F) of various developmental stages. B–D are frozen sections, labeled with MF-20 (red), anti-smooth muscle alpha actin (green) and DAPI (blue). E and F are paraffin-embedded sections, labeled with anti-tropomyosin (red) and DAPI (blue). In A, the head is to the top of the image, dorsal to the right. In B–F, dorsal is to the top of the image and anterior to the right. A: 36 hpf. MF-20 (red) shows that striated myocardium does not extend beyond the outflow portion of the ventricle, the region where the valve will eventually form. Note that the bulbus is not an obvious structure at this early stage of development. B: 5 dpf. C: 8 dpf. D: 13 dpf. At these stages of development, the smooth muscle marker does not label the bulbus (blood cells autofluoresce in the green spectrum). However, neither is there any evidence of striated muscle in the bulbus using MF-20. E: 6 dpf. F: 12 dpf. Anti-tropomyosin confirms the lack of striated myocardium in the bulbus (in these sections, processing for paraffin embedding has eliminated blood cell autofluorescence). Note that the MF-20 and anti-tropomyosin signal adjacent to the bulbus in C–F is derived from skeletal muscle. a—atrium. avc—atrioventricular canal. ba—bulbus arteriosus. sk—skeletal muscle. v—ventricle. Scale bars—100 μm.

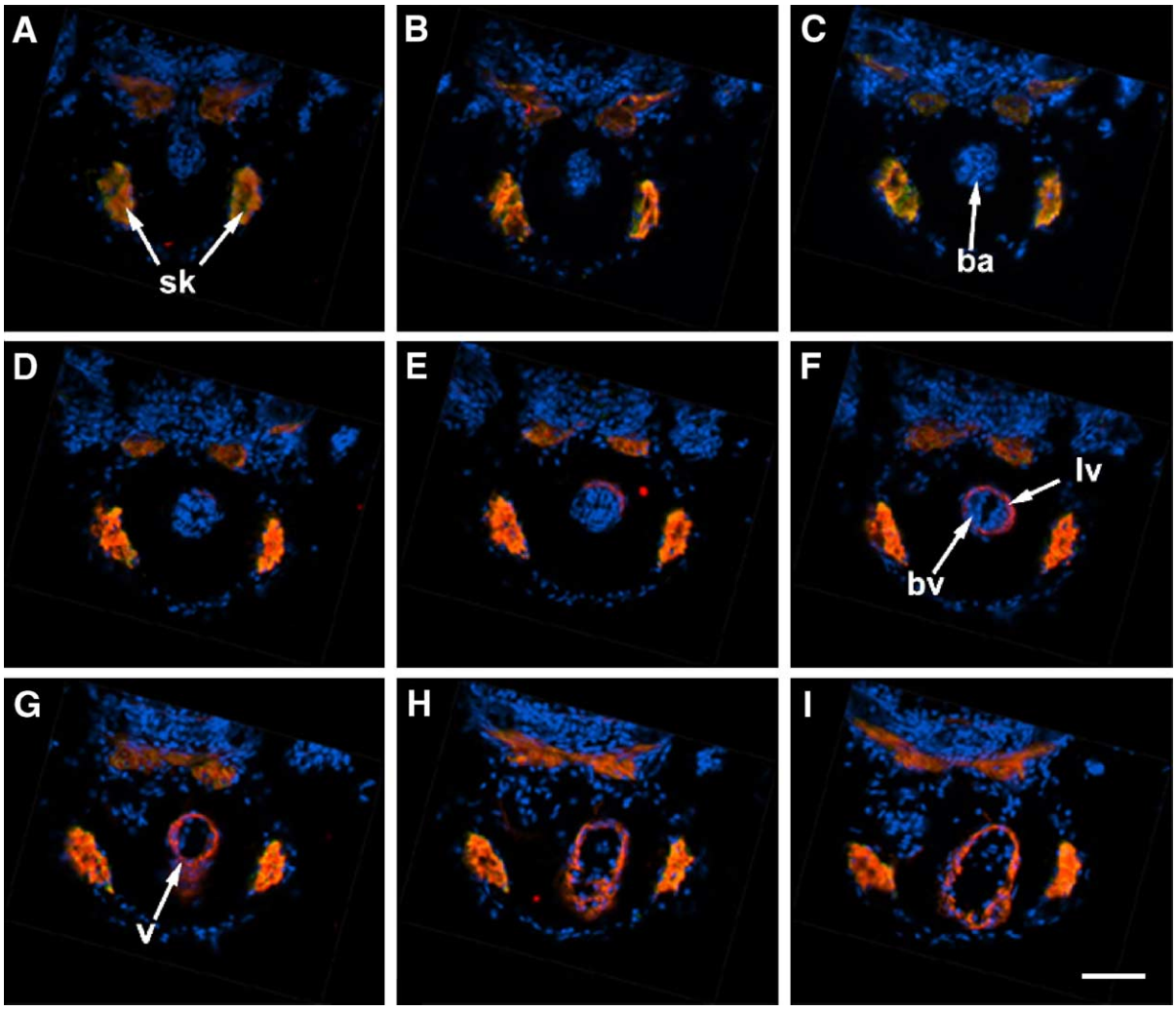


Fig. 3. Striated myocardium does not extend beyond the lip of the ventricle. Serial (anterior to posterior) 8 μm transverse sections through the bulbus arteriosus and ventricle of a 5 dpf embryo. MF-20 (red), DAPI (blue). These images show that there is a narrow band of striated myocardium just distal to the bulboventricular valve (two cusps are seen clearly in F). However, this does not extend into the bulbus. A–C: anterior sections of the bulbus negative for MF-20. Skeletal muscle shows positive labeling. D–F: the striated ring of the 'ventricle lip' becomes apparent close to the valve. G–I: sections immediately posterior to the valve show MF-20-positive labeling in the ventricle. ba—bulbus arteriosus. bv—bulboventricular valve. lv—lip of ventricle. sk—skeletal muscle. v—ventricle. Scale bar—100 μm.

*The bulbus arteriosus is specifically marked by DAF-2DA*

The lack of an effective molecular marker for the zebrafish arterial pole would have made any attempt to characterize its development problematic. However, we have discovered the first bulbus-specific marker, DAF-2DA, and found that it marks the bulbus arteriosus at stages of development when the heart is still undergoing considerable developmental and morphological change. After incubation in a solution of DAF-2DA, fluorescence was observed in the outflow portion of the heart of live fish (Fig. 4A). Although some fluorescence could also be seen in other regions of the embryo, such as the gut and pronephros, strong DAF-2DA reactivity was not observed in any other region of the cardiovascular system. After observation of whole-mount embryos, some were selected for fixation, paraffin embedding and sectioning. Both DAF-2DA- and striated muscle-derived fluorescence was still robust after these procedures. DAF-2DA reactivity in the bulbus was distinct from labeling in the ventricle and atrium (Fig. 4B), and dissected hearts showed clear marker-derived delineation between the ventricle and bulbus (Fig. 4C). In section, DAF-2DA reactivity was observed along the entire length of the bulbus from the outflow portion of the ventricle to the ventral aorta and was confirmed as being distinct from striated muscle labeling in the ventricle (Figs. 4D–I). The localized reactivity of this marker was further confirmation that the bulbus is phenotypically distinct from the atrioventricular regions of the heart.

DAF-2DA labeling of the bulbus was first observed in embryos that had reached approximately 48 hpf, when the outflow portion of the heart is little more than a narrow band of striated myocardium surrounding the lip of the ventricle. Blood passing through this rudimentary vessel can be seen entering the branched arteries leading to what will become the gill arches later in development. The bulbus remained DAF-2DA reactive throughout development and

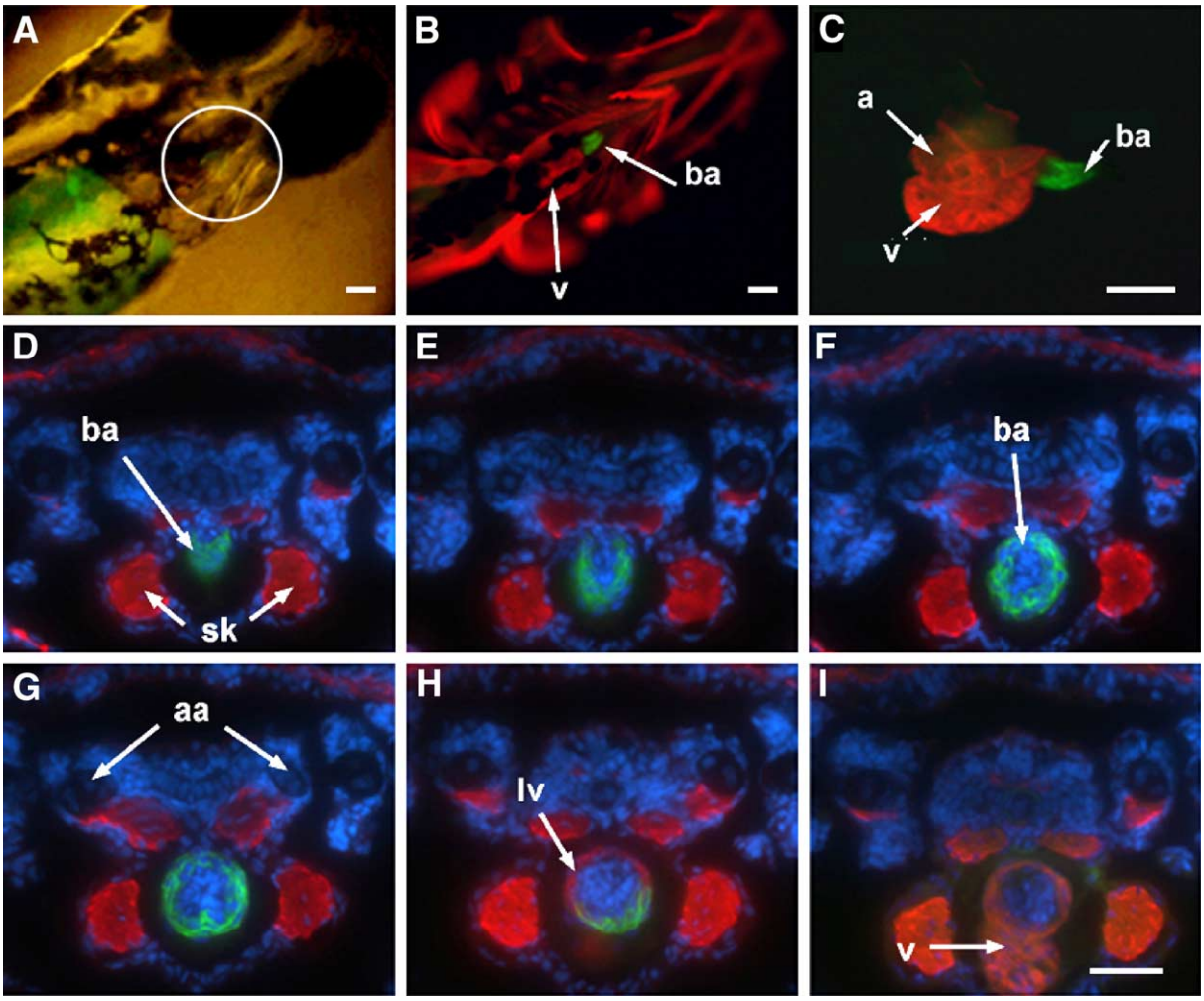


Fig. 4. DAF-2DA and MF-20 label distinct regions of the zebrafish heart. A–C: double-labeled, 5 dpf zebrafish. Scale bars—250 μm. A: ventral view, head is to the top–right. In vivo DAF-2DA labeling. The fluorescent bulbus can be seen in the center of the image (circled), the yolk is also autofluorescing (bottom–left of image). B: similar ventral view to that seen in A, head is to the top–right. DAF-2DA (green) and MF-20 (red) overlay. MF-20 reactivity can be seen in the striated skeletal muscle and in the cardiac muscle of the ventricle. C: lateral view, dorsal to the top, anterior to the right. DAF-2DA and MF-20 overlay of dissected heart shows the clear delineation between bulbal and striated markers. D–I: transverse 8 μm serial sections—anterior to posterior. DAF-2DA, MF-20 and DAPI (blue) staining in 5 dpf zebrafish. Scale bar—100 μm. D: DAF-2DA labeling becomes evident at the tip of the bulbus, close to the ventral aorta. E–G: the bulbus increases in diameter anterior to posterior. H: the DAF-2DA labeled bulbus abuts the MF-20-positive ventricle with no evidence of colocalization in any cells. I: only MF-20-positive myocardium is evident in the ventricle. aa—arch artery. ba—bulbus arteriosus. lv—lip of ventricle. sk—skeletal muscle. v—ventricle.

into adulthood. After 21 dpf, other smooth muscle markers, such as sMLCK, became evident and colocalized with the DAF-2DA domain (Fig. 5), suggesting that it is an early marker of smooth muscle phenotype. In addition, although 21 dpf embryos showed evidence of DAF-2DA reactivity in large blood vessels such as the arch arteries (data not shown), this fluorescence was distinct from that seen in the bulbus and not nearly as intense. It should be noted that another nitric oxide indicator, the red fluorescent diaminorhodamine 4M (DAR-4M AM), also marks the bulbus arteriosus (data not shown).

### *The bulbus does not express cardiac myosin light chain-2*

Because our panel of striated muscle markers also labels skeletal muscle and can cause confusing background signal, we confirmed the absence of a cardiac-specific gene in the bulbus by using *cmlc*2::DsRed2-nuc transgenic fish in which red fluorescent protein (RFP) is expressed under the *cardiac myosin light chain-2* promoter (Mably et al., 2003). In these fish, RFP expression was restricted to the atrium and ventricle and was not expressed in the bulbus at any stage of development (Fig. 6), further demonstrating an obvious delineation between the bulbus arteriosus and the atrioventricular portion of the heart.

### *DAF-2DA also marks the arterial pole of the chick heart*

To ascertain the evolutionary significance of our observations of nitric oxide release in the bulbus, we investigated DAF-2DA reactivity in chick. Fluorescence was observed in the arterial pole of the chick heart after HH stage 23 in a region of nascent smooth muscle known to be added to the base of the common arterial trunk during HH stages 18–22 (Waldo et al.,

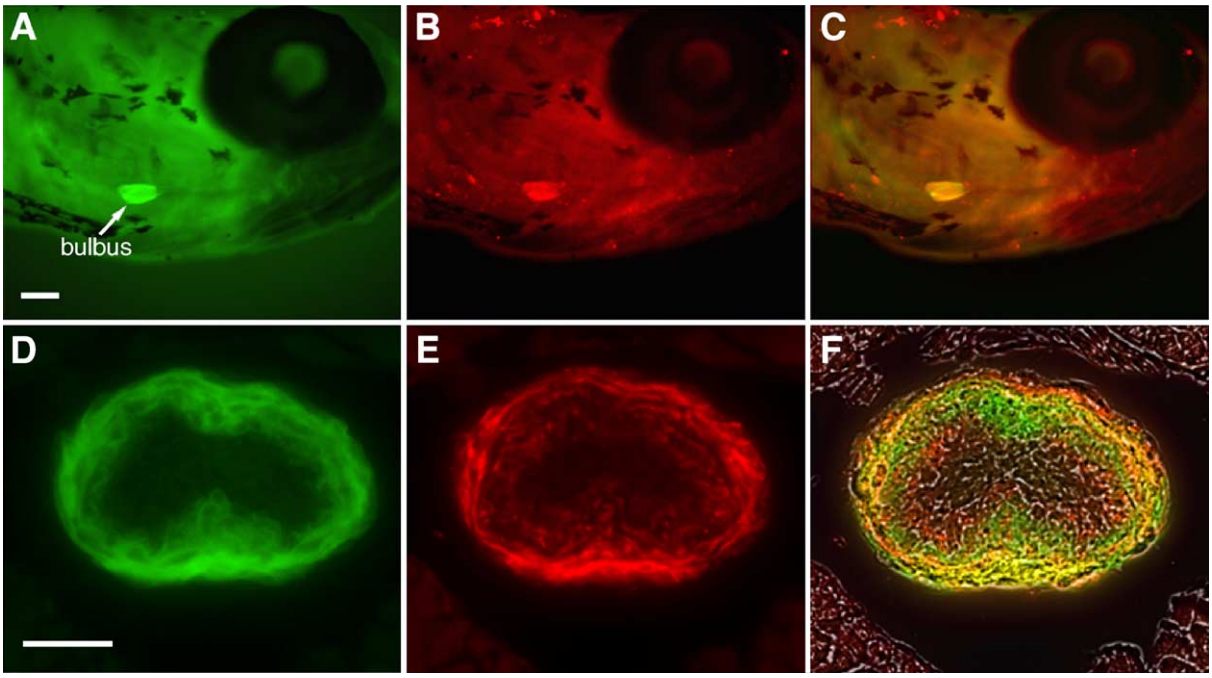


Fig. 5. Anti-sMLCK is the first smooth muscle marker to label the bulbus arteriosus. A–C: lateral view of 21 dpf zebrafish. Head is to the right, dorsal to the top. Scale bar—250 μm. A: DAF-2DA shows strong reactivity in the bulbus. B: the same fish showing anti-sMLCK reactivity. C: overlay image showing colocalization of markers. D–E: transverse section through a 21 dpf bulbus, mid-way between the ventricle and ventral aorta. D: DAF-2DA labeling is restricted to the wall of the bulbus. E: strong sMLCK labeling (red) shows a ring of smooth muscle surrounding the inner subendothelium layer. F: overlay DAF-2DA and sMLCK (on brightfield background) shows colocalization of markers restricted to the wall of the bulbus. Scale bars—50 μm.

2005a,b). Initial reactivity was seen at a time before outflow septation occurs (Figs. 7A–C) and continued until at least HH stage 36 (Figs. 7G–I), when septation is complete and other smooth muscle markers become effective in the chick proximal aorta and pulmonary trunk. Immunolabeling revealed that MF-20 and DAF-2DA are found in overlapping regions of the arterial trunk extending to the truncal–ventricular border. However, as can be seen in Fig. 7F, the myocardium forms a collar around the DAF-2DA reactive cells. Transverse sections confirmed that DAF-2DA and MF-20 label distinct concentric layers of this region of the arterial trunk (Fig. 8). Throughout development, the length of this overlapping region diminishes as the myocardium compacts and regresses towards the ventricle, and by stage 36, when outflow septation is complete, it is limited to a very narrow band just above the semilunar valves (Figs. 7I and 8).

### *The bulboventricular valve is supported by a distinct region of myocardium*

Because there is an overlap of DAF-2DA and MF-20 labeling at the base of the chick arterial pole and because there is some evidence that the conus exists in some teleosts (e.g. Schib et al., 2002), we further investigated the junction of the ventricle and bulbus arteriosus in adult zebrafish. Fig. 9 shows that supporting the bulboventricular valve, there is a region of compact, non-trabeculated myocardium that is rich in collagen and which has a basement membrane staining strongly for laminin. In contrast, laminin is only expressed in the outermost edge of the remainder of the ventricle, and there is less evidence of collagen in the trabeculae. Furthermore, similar to the chick and particularly reminiscent of the staining pattern observed in the chick pulmonary trunk, DAF-2DA and MF-20

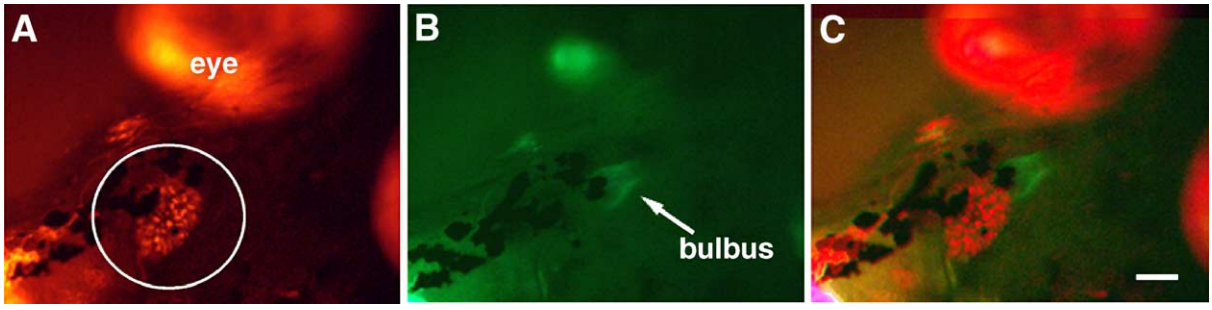


Fig. 6. The bulbus does not express *cardiac myosin light chain-2*. In vivo DAF-2DA staining of a 5 dpf *cmlc*2::DsRed2-nuc transgenic fish. Ventral view, head is to the top–left. Autofluorescence can be seen in the yolk (bottom–left of image) and the eye (top–center). A: red fluorescent protein expressed under the *cmlc-2* promoter is limited to the atrium and ventricle (circled). B: DAF-2DA reactivity in the bulbus. C: overlay image showing obvious phenotypic delineation between the bulbus and other regions of the heart. Scale bar—100 μm.

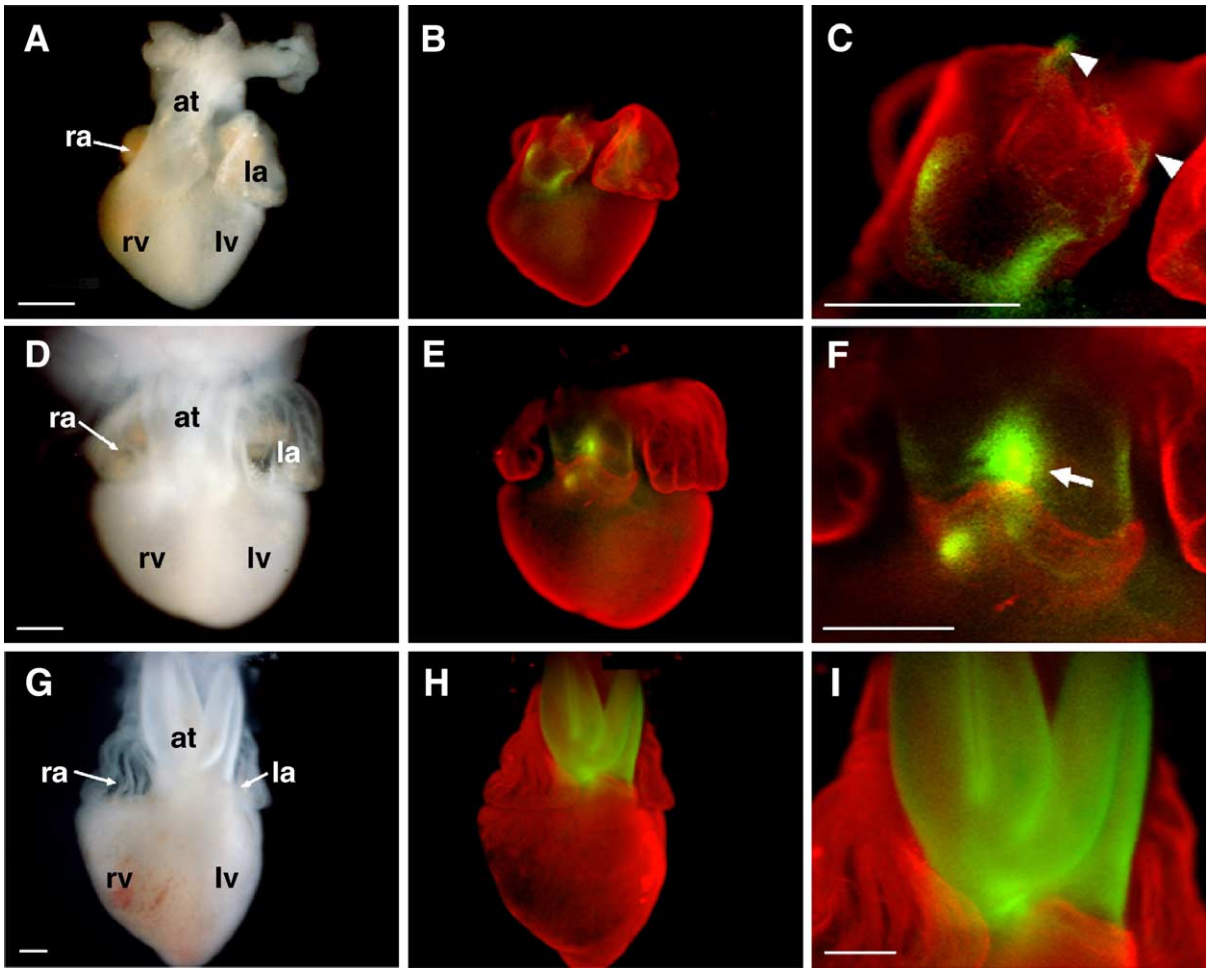


Fig. 7. DAF-2DA reactivity is evolutionarily conserved. DAF-2DA (green) and MF-20 (red) labeling of chick hearts: A: HH stage 26, brightfield image. At this stage, the arterial trunk is a non-septated tube. B: same as in A, showing MF-20 and DAF-2DA labeling. C: enlargement of truncal region in B, showing DAF-2DA reactivity in cells of the arterial trunk beneath the myocardial layer. Some positive cells can also be seen distal to the myocardium (arrowheads). D: HH stage 29, brightfield image. The arterial trunk is now undergoing septation. E: same heart as in D, labeled with MF-20 and DAF-2DA. F: enlargement of DAF-2DA-positive region in E, showing strong reactivity in all regions of the aortic sac, particularly in the region of the outflow septum (arrow) and in the vessel walls. The MF-20-labeled myocardium is undergoing compaction and regression towards the ventricle but still surrounds a region of DAF-2DA-positive cells. G: HH stage 36, brightfield image. Septation is now complete. H: same as in G, showing MF-20 labeling and strong DAF-2DA reactivity in all regions of the arterial trunk. I: enlargement of the DAF-2DA-positive region seen in H. There is now little overlap of the MF-20- and DAF-2DA-positive regions. at—arterial trunk. la—left atrium. lv—left ventricle. ra—right atrium. rv—right ventricle. Scale bars—500 μm.

overlap at the bulboventricular border, such that the myocardium forms a collar around the base of the bulbus and the DAF-2DA reactivity extends down to the roots of the valve leaflets.

## Discussion

The zebrafish is an almost ubiquitously accepted model for comparative biology and has been used extensively for the study of early cardiogenesis. However, much of this research has been concentrated primarily on the development of the atrium and ventricle, at stages long before the bulbus is formed. As a result, this structure has been poorly characterized and, as demonstrated here, undoubtedly misunderstood. In particular, the much-cited and unusual feature of zebrafish development, a striated-to-smooth muscle phenotypic transition in the bulbus, implied that the zebrafish may be poorly suited as a model of conotruncal malformations in human disease. However, we have shown that this enigmatic characteristic was likely based on the misinterpretation of histological and morphological data. This finding has wide-reaching and profound implications, encompassing topics as diverse as evolution, development, anatomy, physiology and human congenital heart defects, and introduces the potential for a paradigm shift in the field of comparative cardiogenesis by allowing the future use of a highly desirable and versatile model in the study of arterial pole development.

Having confirmed that the adult zebrafish bulbus is invested with a considerable volume of smooth muscle, we attempted to follow its development using a panel of immunohistochemical muscle markers and discovered that the muscular phenotype of the bulbus is difficult to characterize in the early embryo. This is because the range of available smooth muscle markers does not react against cells of the bulbus until stages in development after it is already formed. Although such antibodies *will* mark

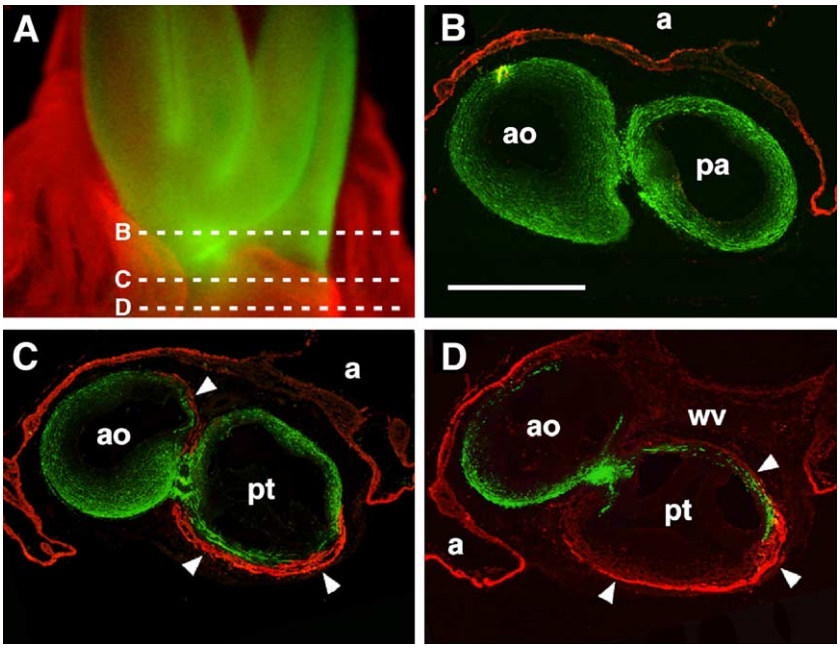


Fig. 8. DAF-2DA and MF-20 label distinct concentric rings in the arterial trunk. Transverse sections through the arterial pole of a stage 36 chick heart, labeled with MF-20 (red) and DAF-2DA (green). Dorsal is to the top of images B through D. A: whole-mount image of arterial trunk showing planes of section in the following images. B: section through the pulmonary artery and aorta above the myocardial trunk. MF-20 labels the atrium. C: plane of section just below the distal limit of myocardium in the pulmonary trunk and aorta, showing clear separation of the concentric MF-20- and DAF-2DA-labeled layers. At this level, there is little myocardium in the aorta compared to the pulmonary trunk (arrowheads). D: plane of section is just above the semilunar valves, the cusps of which can be seen just behind the focal plane. Other than in a small region at the center of the aorticopulmonary septum, the pulmonary trunk is now almost completely surrounded by myocardium (arrowheads). DAF-2DA-positive cells still connect the two arteries and partially line their walls. The wall of the ventricle can now be seen dorsal to the pulmonary trunk and to the right of the aorta. a—atrium. ao—aorta. pa—pulmonary artery. pt—pulmonary trunk. wv—wall of the ventricle. Scale bar—250 μm.

the adult bulbus, none of them is effective at stages of development when it is being added to the heart. This is not a complete surprise, as a similar lack of reactivity has been observed in other models. For example, the same range of smooth muscle markers does not label the chick proximal aorta and pulmonary trunk until advanced stages of outflow septation (Waldo et al., 2005a,b). While this lack of an effective marker may have hindered our attempts to characterize a phenotypic change, we discovered in all embryos examined (from 24 hpf through to over 30 dpf) that our panel of striated muscle markers never actually marked the bulbus either. We have therefore concluded that, although a portion of the arterial pole of the zebrafish heart is indeed striated during early development, this is not what will become the bulbus, a structure that appears to be added to the heart after the atrium and ventricle are already formed and which does not declare itself as muscle of any variety until much later in development. What was previously described as the 'striated bulbus' was undoubtedly the very narrow band of myocardium between the region of the bulboventricular valve and the bulbus per se.

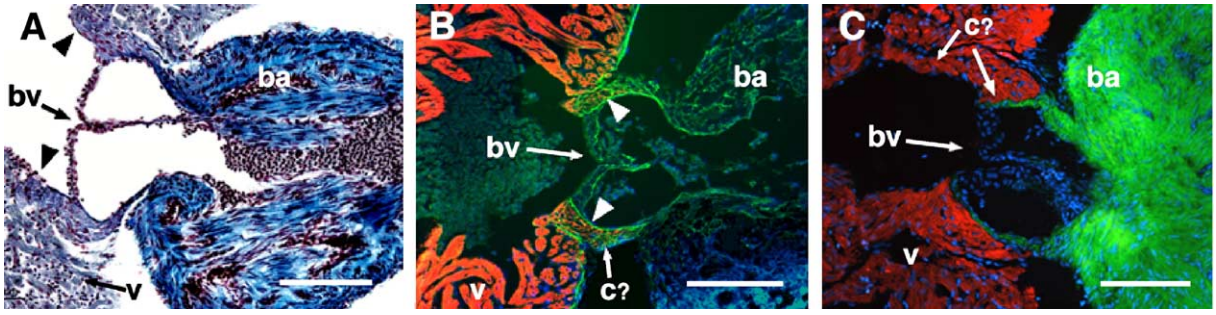


Fig. 9. The bulboventricular valve is supported by a distinct region of myocardium. Longitudinal sections through the zebrafish arterial pole. Cranial to the right of the images. A: hematoxylin and eosin/Mallory's trichrome stain. The bulbus arteriosus is highly collagenous, indicated by the intense blue staining. The myocardium supporting the valve stains more strongly blue than the ventricle, particularly at the lumenal edge, and is both compact and non-trabeculated. Note that the non-trabeculated myocardium extends a considerable distance caudal to the valve (black arrowheads). B: anti-laminin (green), MF-20 (red) and DAPI (blue). The MF-20-positive tissue supporting the valve clearly includes striated muscle (white arrowheads). However, this region also stains intensely for laminin, demonstrating its distinctive character in comparison to the trabeculated myocardium of the ventricle. C: DAF-2DA (green), MF-20 (red) and DAPI (blue). DAF-2DA labels the bulbus and lumenal edge of the tissue supporting the valve, while the outer edge is MF-20-positive. However, it does not label the myocardium on the caudal (ventricular) side of the valve. ba—bulbus arteriosus. bv—bulboventricular valve. c—conotruncus? v—ventricle. Scale bar—250 μm.

The study of the development of the teleost bulbus arteriosus remains controversial. Evolutionarily, it is generally accepted that the conus, a prominent structure found in the elasmobranchs (sharks, skates and rays) and lined with several rows of valves, diminished in size as the bulbus developed in the bony fishes (Guerrero et al., 2004; Schib et al., 2002; Farrell and Jones, 1992; Satchell, 1991). In many cases, it has been assumed that the teleost conus remains as either a vestigial structure or has actually disappeared completely as a consequence of the progressive development (physical and functional) and dramatic increase in size of the bulbus. We have found that the region of myocardium at the lip of the ventricle, which surrounds and supports the bulboventricular valve, is phenotypically distinct from the myocardium in the remainder of the ventricle, as it is more collagenous and stains intensely for laminin (Fig. 9). This region of the zebrafish arterial pole appears strikingly similar to the pulmonary trunk and infundibulum of the chick, as there are concentric rings of distinct tissue above the valve and clearly a stretch of non-trabeculated myocardium below, suggesting that there may be a vestigial conotruncus in the zebrafish. Thus, our work supports the assertions of Guerrero et al. (2004) and Schib et al. (2002), who have clearly demonstrated the presence of the conus in the sturgeon (*Acipenser naccarii*) and the gilthead seabream (*Sparus auratus*), respectively, and have suggested that a review of the assumed disappearance of the teleost conus may be necessary (Guerrero et al., 2004). However, Guerrero et al. (2004) still propose a developmental transition from striated to smooth muscle in the bulbus, an interpretation of data that was likely based on the assumption that such a transition occurs in the zebrafish. A simpler explanation of their observations is a craniocaudal growth of the bulbus as the conus compacts or regresses towards the ventricle over developmental time. Our work should provide a foundation that will allow a reassessment and clarification of some of these issues.

In our attempts to further an understanding of the outflow region of the zebrafish heart, we have discovered that DAF-2DA, a fluorescent nitric oxide indicator, specifically marks the zebrafish bulbus arteriosus from approximately 48 hpf and to adulthood. It is therefore effective through stages of development during which the arterial pole of the zebrafish heart is changing from a simple narrow band of striated muscle around the lip of the ventricle (where the bulboventricular valve will form) to the more easily distinguishable, elongated, bulbal structure seen in the juvenile (and adult) fish. Furthermore, this is a time during which the atrioventricular portion of the heart is undergoing considerable morphological alteration. After 2 days of development, a considerable volume of yolk remains, so the heart is curved around the frontal surface of the yolk-sac and lies almost perpendicular to the craniocaudal axis. Although beginning to loop, the atrium and ventricle are still laterally adjacent, with the atrium lying more ventrally and slightly more caudally within the pericardial cavity. Over the next 48 h, the volume of yolk diminishes as it is partially absorbed, such that the heart begins to align along the craniocaudal axis. The bulbus extends craniocaudally and increases considerably in diameter. The heart continues to loop, with the atrium rotating towards the right and dorsally, ultimately to adopt a position directly above the ventricle. Importantly, DAF-2DA labeling of the bulbus is robust throughout these morphological changes and continues beyond a time at which the heart becomes essentially fully formed. DAF-2DA is limited to tissues of the bulbus arteriosus and does not mark any other region of the heart. We have therefore discovered the first highly specific marker for the outflow portion of the zebrafish heart and demonstrated its utility and versatility in various experimental protocols conducted during important developmental stages of this model species.

DAF-2DA is an unusual marker as it simply indicates the presence of a small cell-signaling molecule, NO, within the cytoplasm, rather than binding to a structural or functional protein such as is the case for many other markers. Under normal circumstances, NO is short lived within cells, but reaction with the DAF-2DA-hydrolyzed product, DAF-2, results in an accumulation of the fluorescent adduct, DAF-2T. This effectively cages NO within the cytoplasm, and the resulting fluorescence is thus indirectly indicative of the level of NO production within the cell.

Since the identification of NO as an ‘endothelial-derived relaxation factor’ in the 1980s (Furchgott and Zawadski, 1980; Ignarro et al., 1987), its multi-functional importance and almost ubiquitous presence as a novel signaling molecule has become evident. It has been implicated in the regulation of various activities in organs, such as the brain, liver, kidneys, stomach and heart, and in the ability of the immune system to mount an effective response against viral, bacterial and parasitic infections and tumors. With specific regard to the cardiovascular system, the vasodilatory effects of NO originally described by Furchgott and Zawadski (1980) are now known to exert a strong control on circulation and blood pressure by acting on arterial and vascular smooth muscle cells. In addition, NO protects the blood vessels by inhibiting vascular smooth muscle proliferation and contraction and by preventing leukocyte adhesion and the aggregation of platelets (Albrecht et al., 2003; Gewaltig and Kojda, 2002). It has been shown that the venous and arterial vasculature of zebrafish larvae is responsive to endogenously produced NO (Fritsche et al., 2000), so the fact that the zebrafish bulbus arteriosus produces high levels of NO is intriguing. Further analysis of the phenomenon may lead to a better understanding of the development, physiology and function of this structure.

In other species, the requirement for NO in development is well established. For example, *Drosophila* has a single nitric oxide synthase gene (*dNOS*), known to be involved in the development of the imaginal discs in the embryo and responsible for the control of cell proliferation. A mutation in *dNOS* that renders the enzyme inactive results in lethality at late embryonic and larval stages (Regulski et al., 2004). In contrast, there would appear to be some functional redundancy between the three nitric oxide synthases found in mammals, and although a triple loss-of-function phenotype has not been established, mice in which two of these genes have been ablated show drastically reduced viability (Huang et al., 1993, 1995). In the embryonic heart, certain developmental process-

es, including remodeling of the outflow tract, are directed by cues such as hypoxia (Sugishita et al., 2004) and shear stress forces (Groenendijk et al., 2004; Hove et al., 2003). As NO is implicated in the vascular response to hypoxia (Ignarro et al., 1987) and as the promoter for the endothelial nitric oxide synthase gene (*e-NOS*) contains a sheer stress-responsive element (Groenendijk et al., 2004), it seems intuitive that NO is necessary for the normal cardiogenic program. Furthermore, one could speculate that, as the teleost bulbus is particularly hypoxic, lying at the very limit of the vasculature before blood is oxygenated at the gills, this may account for the early and strong response of NO release. Thus, as the gills are being formed and the highly elastic bulbus is growing to prevent back-flow and to protect the gills from fluctuations in blood pressure, NO release likely induces dilatation of the vessel and provides a means by which a uniform blood flow to the gills is ensured.

Regardless of its nature in zebrafish, we have shown that DAF-2DA is specifically localized to the bulbus, in addition to a limited number of organs not associated with the cardiovascular system. Importantly, it is not seen in any other region of the heart during development and therefore allows the cells of the bulbus to be visually segregated from those of the ventricle and atrium. In addition, the fact that at later stages of development, DAF-2DA reactivity colocalizes with known markers of smooth muscle, such as anti-myosin light chain kinase, suggests that it is an early marker of smooth muscle phenotype. As further evidence of this, we have shown that DAF-2DA also labels the arterial pole of the chick heart from stages of development before smooth muscle markers are effective but in regions that ultimately adopt a smooth muscle phenotype. For example, DAF-2DA reactivity in Figs. 7H–I and in Fig. 8 supports the observations of Waldo et al. (2005b), who showed that, at day 11 of development (HH stage 37), smooth muscle extends to the semilunar valves at the base of the pulmonary trunk and aorta and is surrounded by the myocardial wall. Importantly, while we cannot claim definitively that DAF-2DA is marking smooth muscle in early development, as we are unable to show its colocalization with known markers in fish younger than 21 dpf, the fact that it labels the bulbus from its earliest development through to adulthood is clearly indicative that the bulbus is always phenotypically distinct from the myocardium.

Intriguingly, the fact that DAF-2DA also marks the arterial pole of the chick heart strongly suggests that this is a conserved developmental or physiological phenomenon. More importantly, the region marked by DAF-2DA in chick is not considered to be part of any heart chamber and is among the tissues added to the heart from the secondary heart field. Could this be the first tantalizing evidence for the presence of a secondary heart field in the zebrafish? Whether or not this proves to be the case, we are confident that we have provided evidence that the zebrafish bulbus arteriosus has been wrongly designated as a heart chamber and is actually more homologous to the aortic trunk of higher vertebrates.

In conclusion, this work has effectively solved an enigma by showing that a previously reported striated-to-smooth muscle phenotypic change does not occur. Thus, the zebrafish may after all be similar to other models of cardiogenesis and may be well suited for the study of arterial pole development and conotruncal malformations. A greater appreciation of this hitherto neglected aspect of zebrafish cardiogenesis may help to eliminate the confusion that pervades this area of research and lead to a greater understanding about the development of the arterial pole of the vertebrate heart.

## Acknowledgments

We thank Dr. Mary Redmond Hutson for help with imaging of sections. We are grateful to Dr. Debbie Yelon and Heidi Auman at the New York University Medical Center for sharing initial observations of DAF-2DA reactivity close to the zebrafish heart. Thanks to the entire Kirby laboratory group for invaluable support. This work was supported by grants from NIH HL-36059, HL-70140, HD-39946, and a Duke Environmental Health Science Research Center Grant to M.L.K.

## References

Albrecht, E.W., Stegemen, C.A., Heeringa, P., Henning, R.H., van Goor, H., 2003. Protective role of endothelial nitric oxide synthase. J. Pathol. 199, 8–17.

Arguëllo, C., Delacruz, M.V., Sanchez, C., 1978. Ultrastructural and experimental evidence of myocardial cell differentiation into connective tissue cells in embryonic chick heart. J. Mol. Cell. Cardiol. 10, 307–315.

Bader, D., Masaki, T., Fischman, D.A., 1982. Immunochemical analysis of myosin heavy chain during avian myogenesis in vivo and in vitro. J. Cell Biol. 95, 763–770.

Bone, Q., Marshall, N.B., Blaxter, J.H.S., 1999. Biology of Fishes. Stanley Thornes, Cheltenham, UK.

Epstein, F.H., Epstein, J.A., 2005. A perspective on the value of aquatic models in biomedical research. Exp. Biol. Med. 230, 1–7.

Farrell, A.P., Jones, D.R., 1992. The heart. In: Hoar, W.S., Randall, D.J., Farrell, A.P. (Eds.), Fish Physiology, The Cardiovascular System, Part A, vol. XII. Academic Press, San Diego, pp. 1–87.

Fishman, M.C., Chien, K.R., 1997. Fashioning the vertebrate heart: earliest embryonic decisions. Development 124, 2099–2117.

Fritsche, R., Schwerte, T., Pelster, B., 2000. Nitric oxide and vascular reactivity in developing zebrafish, *Danio rerio*. Am. J. Physiol.: Regul., Integr. Comp. Physiol. 279, R2200–R2207.

Furchgott, R.F., Zawadski, J.F., 1980. The obligatory role of endothelial cells in the relaxation of arterial smooth muscle by acetylcholine. Nature 288, 373–376.

Gewaltig, M.T., Kojda, G., 2002. Vasoprotection by nitric oxide: mechanisms and therapeutic potentials. Cardiovasc. Res. 55, 250–260.

Goodrich, E.S., 1930. Studies on the Structure and Development of Vertebrates. Macmillan, London.

Groenendijk, B.C.W., Hierck, B.P., Gittenberger-de Groot, A.C., Poelmann, R.E., 2004. Development-related changes in the expression of shear stress responsive genes *KLF-2, ET-1*, and *NOS-3* in the developing cardiovascular system of chicken embryos. Dev. Dyn. 230, 57–68.

Guerrero, A., Icardo, J.M., Duran, A.C., Gellego, A., Domezain, A., Colvee, E., Sans-Coma, V., 2004. Differentiation of the cardiac outflow tract components in alevins of the sturgeon *Acipenser naccarii* (Osteichthyes, Acipenseriformes): implications for heart evolution. J. Morphol. 260, 172–183.

Hamburger, V., Hamilton, H.L., 1951. A series of normal stages in the development of the chick embryo. J. Morphol. 88, 49–92.

Hickman, C.P., Roberts, L.S., Hickman, F.M., 1988. Integrated Principles of Zoology. Times Mirror/Mosby College Publishing, St. Louis.

Hove, J.R., Koster, R.W., Forouhar, A.S., Acevedo-bolton, G., Fraser, S.E., Gharib, M., 2003. Intracardiac fluid forces are an essential epigenetic factor for embryonic cardiogenesis. Nature 421, 172–177.

Hu, N., Sedmera, D., Yost, J., Clark, E.B., 2000. Structure and function of the developing zebrafish heart. Anat. Rec. 260, 148–157.

Hu, N., Yost, H.J., Clark, E.B., 2001. Cardiac morphology and blood pressure in the adult zebrafish. Anat. Rec. 264, 1–12.

Huang, P.L., Dawson, T.M., Bredt, D.S., Snyder, S.H., Fishman, M.C., 1993. Targeted disruption of the neuronal nitric oxide synthase gene. Cell 75, 1273–1286.

Huang, P.L., Huang, Z., Mashimo, H., Bloch, K.D., Moskowitz, M.A., Bevan, J.A., Fishman, M.C., 1995. Hypertension in mice lacking the gene for endothelial nitric oxide synthase. Nature 377, 239–242.

Ignarro, L.J., Buga, G.M., Wood, K.S., Byrns, R.E., Chadhuri, G., 1987. Endothelium-derived relaxing factor produced and released from artery and vein is nitric oxide. Proc. Natl. Acad. Sci. U. S. A. 84, 9265–9269.

Keegan, B.R., Meyer, D., Yelon, D., 2004. Organization of cardiac chamber progenitors in the zebrafish blastula. Development 131, 3081–3091.

Kimmel, C.B., Ballard, W.B., Kimmel, S.R., Ullman, B., Schilling, T.F., 1995. Stages of embryonic development of the zebrafish. Dev. Dyn. 203, 253–310.

Kojima, H., Nakatsubo, N., Kikuchi, K., Kawahara, S., Kirino, Y., Nagoshi, H., Hirata, Y., Nagano, T., 1998. Detection and imaging of nitric oxide with novel fluorescent indicators: diaminofluoresceins. Anal. Chem. 70, 2446–2453.

Lawson, R., 1979. The comparative anatomy of the circulatory system. In: Wake, M.H. (Ed.), Hyman's Comparative Vertebrate Anatomy, 3rd ed. University of Chicago Press, Chicago, pp. 448–554.

Mably, J.D., Mohideen, M.A.P.K., Burns, C.G., Chen, J.N., Fishman, M.C., 2003. *Heart of glass* regulates the concentric growth of the heart in zebrafish. Curr. Biol. 13, 2138–2147.

McCauley, W.J., 1971. Vertebrate Physiology. W.B. Saunders Company, Philadelphia.

Nusslein-Volhard, C., Dahm, R. (Eds.), 2002. Zebrafish. Practical Approach. Oxford Univ. Press, Oxford.

Orr, R.T., 1982. Vertebrate Biology, 5th ed. Saunders College Publishing.

Regulski, M., Stasiv, Y., Tully, T., Enikolopov, G., 2004. Essential function of nitric oxide synthase in *Drosophila*. Curr. Biol. 14, 881–882.

Rothenberg, F., Fisher, S.A., Watanabe, M., 2003. Sculpting the cardiac outflow tract. Birth Defects Res., Part C 69, 38–45.

Satchell, G.H., 1991. Physiology and Form of Fish Circulation. Cambridge Univ. Press, Cambridge.

Schib, J.L., Icardo, J.M., Duran, A.C., Guerrero, A., Lopez, D., de Andres, A.V., Sans-Coma, V., 2002. The conus arteriosus of the adult gilthead seabream (*Sparus auratus*). J. Anat. 201, 395–404.

Schmidt-Nielsen, K., 1997. Animal Physiology, 5th ed. Cambridge Univ. Press, Cambridge.

Simões, K., Vicentini, C.A., Orsi1, A.M., Cruz, C., 2002. Myoarchitecture and vasculature of the heart ventricle in some freshwater teleosts. J. Anat. 200, 467–475.

Stainier, D.Y.R., Lee, R.K., Fishman, M.C., 1993. Cardiovascular development in the zebrafish: I. Myocardial fate map and heart tube formation. Development 119, 31–40.

Sugishita, Y., Watanabe, M., Fisher, S., 2004. Role of myocardial hypoxia in the remodeling of the embryonic avian cardiac outflow tract. Dev. Biol. 267, 294–308.

Waldo, K.L., Hutson, M.R., Stadt, H.A., Zdanowicz, M., Zdanowicz, J., Kirby, M.L., 2005a. Cardiac neural crest is necessary for normal addition of the myocardium to the arterial pole from the secondary heart field. Dev. Biol. 281, 66–77.

Waldo, K., Hutson, M.R., Ward, C.C., Zdanowicz, M., Stadt, H.A., Kumiski, D., Abu-Issa, R., Stadt, H.A., Kirby, M.L., 2005b. Secondary heart field contributes myocardium and smooth muscle to the arterial pole of the developing heart. Dev. Biol. 281, 78–90.

Watanabe, M., Choudry, A., Berlan, M., Singal, A., Siwik, E., Mohr, S., Fisher, S.A., 1998. Developmental remodeling and shortening of the cardiac outflow tract involves myocyte programmed cell death. Development 125, 3809–3820.

Westerfield, M., 1993. The Zebrafish Book. University of Oregon Press, Eugene, OR.

Ya, J., van den Hoff, M.J.B., de Boer, P.A.J., Tesink-Taekema, S., Franco, D., Moorman, A.F.M., Lamers, W.H., 1998. The normal development of the outflow tract in the rat. Circ. Res. 82, 464–472.

Young, J.Z., 1981. The Life of Vertebrates, 3rd ed. Clarendon Press, Oxford.